Subwavelength transportation of light with atomic resonances

Siu-Tat Chui,[1] Shengwang Du,[2] and Gyu-Boong Jo[2,*]

[1]*Bartol Research Institute and Department of Physics and Astronomy, University of Delaware, Newark, Delaware 19716, USA*

[2]*Department of Physics, The Hong Kong University of Science and Technology, Clear Water Bay, Kowloon, Hong Kong, China*

(Received 1 June 2015; published 9 November 2015)

We propose and investigate a type of optical waveguide made by an array of atoms without involving conventional Bragg scattering or total internal reflection. A finite chain of atoms collectively coupled through their intrinsic resonance supports a propagating mode with minimal radiative loss when the array spacing a is around $0.6\lambda_0/2\pi$ where λ_0 is the wavelength of the nearly resonant optical transition. We find that the transportation is robust with respect to position fluctuation and remains possible when the atoms are placed on a circle. Our result paves the way to implement the subwavelength transportation of light in integrated optical circuits with cold atoms.

DOI: 10.1103/PhysRevA.92.053826 PACS number(s): 42.82.Et, 67.85.−d, 78.67.Pt

I. INTRODUCTION

There is much recent development of integrated optical circuits localizing and interfacing cold atoms in which quantum networks, quantum many-body physics, and quantum optics can be explored [1–5]. This new interdisciplinary toolbox ranging from atomic physics and quantum optics to nanophotonics opens a new door to investigate a wide range of remarkable phenomena such as the coherent transportation of photons emitted from an atom [6,7] and atomic mirrors [8]. In this article, we examine a subwavelength waveguide made with an array of atoms along linear and circular geometries. As is reviewed recently [9], subwavelength phenomenon has been extensively exploited in free-space birefringence optics [10], polarizers [11,12], and antireflection surfaces [13,14]. These structures are employed to optimize fiber-chip grating couplers [15], vertical-cavity surface-emitting lasers (VCSELs) [16], and wavelength multiplexers [17]. Furthermore, low-loss waveguide crossings [18], high Q factor resonators [19], and ultrabroadband multimode interference (MMI) couplers [20] are demonstrated in subwavelength structures.

In parallel, nanoscale waveguides that confine, guide, and manipulate the electromagnetic energy on subwavelength scales have been actively studied as optoelectronic circuits [21–23]. The plasmon-based waveguides such as those made with nanowires or metallic particles [24–29] have very excellent lateral confinement but the propagation distance is considerably limited. This originates from the intrinsic loss of the metal which hampers the implementation of nanoscale metal plasmon waveguides. This loss is reduced when dielectric scatterers are used [30] via so-called "geometric resonances." For scatterers with size R, however, the geometric resonance strictly requires the lattice spacing a satisfying $2R < a < \lambda/2$ where λ is the wavelength of the guided light. Thus, the finite size R of the scatterer considerably limits the flexibility of the waveguide made by scatterers. It has not been possible to demonstrate waveguides with arbitrary curvature from rigorous first-principles numerical calculations. Nor are the waveguiding properties of simple arrays of scatterers robust under positional fluctuations.

Here, we consider a waveguide made with an array of atoms where there is no size restriction. Instead of the "geometric resonance" with dielectric scatterers, we employ intrinsic "atomic resonance" to support a propagating mode in flexible subwavelength geometries in this article. With appropriate lattice spacing $a \sim 0.6\lambda_0/2\pi$ of the atomic chain where λ_0 denotes the wavelength of nearly resonant light, the *external* electric field exciting the first few atoms can propagate along the finite size of the chain with minimal radiation loss. We find that the transportation is robust with respect to the position fluctuation of atoms and is possible when the atoms are placed on a circle. The recent development of plasmonic nanosphere [31] or two-dimensional photonic crystals [32] localizing atoms should allow one to prepare an array of atoms with tunable lattice spacing. Indeed, the new mechanism of optical waveguide mode examined in this work requires an intrinsic atomic resonance so that it could be readily adopted in a system of artificial atoms (e.g., quantum dots) [33] or an array of superconducting circuits [34].

Through the excitation in an atom at one end of the chain, energy is transferred to all adjacent atoms in turn through the resonant excitations. For the chain of atoms, resonant excitations in different atoms are coupled by electromagnetic interaction and form collective optical modes. We consider the transportation of this excitation along the atomic chain is through an intrinsic p-wave resonance. Then, we investigate how excitation of the first atom by an external electric field $\mathbf{E}$ can travel down the chain.

II. WAVEGUIDE MODE IN A CHAIN OF ATOMS

We expand the field near each atom locally in terms of vector spherical harmonics and examine the scattering phase shift of electric fields from each atom as is described in Appendix A. To identify the waveguide mode along the chain of atoms, we employ the multiple scattering theory describing electromagnetic interactions between the different atoms [35]. Here, the scattered electric field from a single atom is related to the sum of the external electric field and the scattered fields from all the other atoms. As we see below, the waveguide mode is indicated by the undiminished propagation of the electromagnetic wave down the chain after the first few atoms are excited.

*gbjo@ust.hk

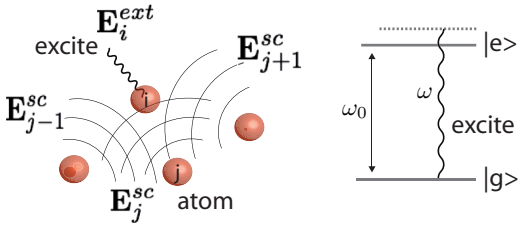

FIG. 1. (Color online) Our modeled system. An array of two-level atoms responding to the external electromagnetic field $E_i^{\rm ext}$ at the frequency of ω. The ith atom is driven by both external fields and scattered fields $E_j^{\rm sc}$ from jth atoms where $j \neq i$.

In the multiple scattering approach [35], the total incoming electric field driving the ith atom $\mathbf{E}_i^{(1)}$ is the sum of the external electric field $\mathbf{E}_i^{\rm ext}$ and the scattered fields from all the other atoms: $\sum_{j\neq i}\mathbf{E}_{ij}^{\rm (sc)}$, i.e., $\mathbf{E}_i^{(1)} = \mathbf{E}_i^{\rm ext} + \sum_{j\neq i}\mathbf{E}_{ij}^{\rm (sc)}$ as is illustrated in Fig. 1. This incoming field is scattered by the atom and produces a scattered field $\mathbf{E}_i^{(3)}$ that is equal to the $\mathbf{t}$ matrix times the incoming field: $\mathbf{E}_i^{(3)} = \mathbf{t}\mathbf{E}_i^{(1)}$. The field $\mathbf{E}_{ij}^{\rm (sc)}$is equal to the photon propagator $\mathbf{G}_{ij}$ times the scattered field from site $\mathbf{j}$: $\mathbf{E}_{ij}^{\rm (sc)} = \mathbf{G}_{ij}\mathbf{E}_j^{(3)}$. Here, the $\mathbf{t}$ matrix is diagonal due to the rotational invariance of the Hamiltonian (see Appendix B for details), and given by $t = \tan\delta/(\tan\delta + i)$ where the scattering phase shift satisfies $\tan\delta = 1/(\omega - \omega_0 + i\Gamma)$ for the natural linewidth Γ of the optical transition. To summarize, we get the set of linear equations

$$\mathbf{E}_i^{(3)} = \mathbf{t}_i\left[\sum_{j\neq i}\mathbf{G_{ij}}\mathbf{E_j^{(3)}} + \mathbf{E}_i^{\rm ext}\right]. \tag{1}$$

In momentum space, the multiple scattering equation

$$\mathbf{E}^{(3)}(k) = \frac{\mathbf{E}^{\rm ext}(k)}{1 - \mathbf{t(k)G(k)}} \tag{2}$$

gives the resonance condition $\mathbf{t(k)G(k)} = \mathbf{1}$. For a finite system, the possible wave vectors form a discrete set. The real solutions to this equation provide for truly one-dimensional "photonic band" states, examples of which have been discussed previously [30]. This provides for the waveguide modes.

A. Linear chain

To illustrate the subwavelength transport of photons, we first consider a one-dimensional array of 30–320 atoms with a p-wave resonance at an angular frequency ω_0 and separated by lattice spacings a. The steady-state distribution of the electric field as a function of the position of the atoms is numerically calculated when the first few atoms are excited by the external electric field. We find that there can be a large response at the end of the chain but only when the external field is perpendicular to the line of atoms. We attribute this to the nature of p-wave resonance of atoms. In addition, we investigate the dependence on the way the system is excited. The propagated waveguide mode at the end of the chain does not show significant difference for two cases—when the first or the first few atoms are excited—as long as the length of the chain is much longer than the wavelength λ_0. For the rest of the part, we consider the case when only the first atom is externally excited.

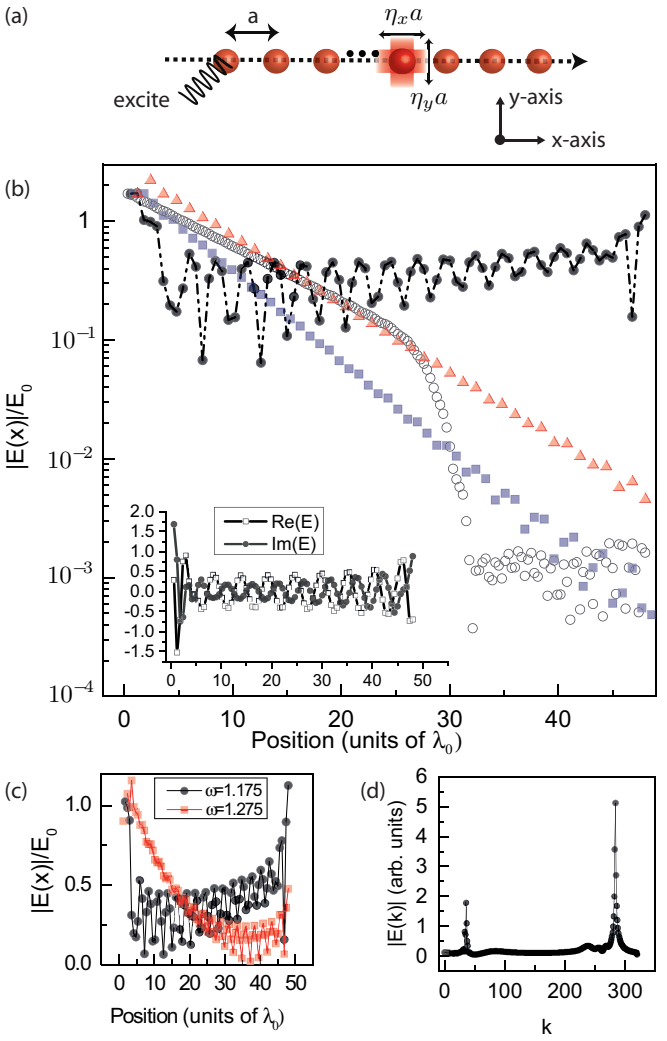

FIG. 2. (Color online) Waveguide mode along the linear chain of atoms. (a) An array of atoms is placed on a straight line with the separation of a. Here, the amount of position fluctuations is indicated by $\eta_{x,y}a$. (b) The normalized intensity of the electric field $|E|$ is shown as a function of the position of atoms for different lattice spacing $a = 0.3\lambda_0/2\pi$ (open circle), $a = 0.6\lambda_0/2\pi$ (solid circle), $a = 0.9\lambda_0/2\pi$ (solid triangle), and $a = 1.2\lambda_0/2\pi$ (solid square). Here, E_0 is the amplitude of the external electric field exciting the first few atoms. The inset shows the real and imaginary parts of the electric field for the propagating mode when $a = 0.6\lambda_0/2\pi$. (c) Distribution of the electric field as a function of the position is shown for different incoming angular frequency normalized by E_0. (d) Fourier transform of the electric field in the transverse mode along the propagating direction (x) as a function of the wave vector $\mathbf{k}$ in units of $2\pi/(aN)$ for $N = 320$ atoms on a straight line of lattice spacing $a = 0.6\lambda_0/2\pi$. The amount of power transported can be estimated from the Poynting vector from the sum of the scattered wave of all the atoms along the chain (see Appendix D).

Our numerical calculation suggests that the waveguide mode can be achieved for a spacing $a \sim 0.6\lambda_0/2\pi$. Since the resonance is intrinsic in the atomic system, the wavelength of resonant light λ_0 is species specific. In Fig. 2 we show the

electric field magnitude, normalized by external electric field amplitude E_0, as a function of the position in the unit of λ_0 for different lattice spacing a. Only for a around $0.6\lambda_0/2\pi$ is there a "waveguide" mode. For the other array spacing, the wave is nonpropagating down the chain. The real part and the imaginary part of the field as a function of atom position are compared in the inset of Fig. 2(b). As expected, they are of comparable magnitude and exhibit the same spatial dependence. This figure illustrates that the wave is a product of two terms, one slowly varying and the other periodic and rapidly varying (carrier wave).

B. Waveguide condition

Let $k_\perp$ be the transverse wave vector normal to the propagation direction. To suppress the radiation loss, $k_\perp$ must be imaginary. The transverse wave vector $k_\perp$ is given by $k_\perp = \sqrt{(2\pi/\lambda)^2 - k_x^2}$, with λ the wavelength of the guided wave and k_x the wave vector along propagation direction. The Fourier transform of the electric field, $E(k) = \sum_j E_j \exp(ikja)/\sqrt{N}$, in the transverse mode is shown as a function of the wave vector k in units of $2\pi/(Na)$ for $N = 320$ atoms [see Fig. 2(d)]. The incoming wave has a wave vector $k_i = \omega Na/(2\pi c) = 35.9$ in the present unit. This is much less than the dominant peak at $k = 284$ and therefore k_y is imaginary. This large periodicity is mainly due to the "carrier wave," which sustains the subwavelength transport. There is another peak in the Fourier transform at k_i, which reflects the contribution from atoms at the beginning of the chain.

As k_x takes its maximum at the Brillouin zone boundary $K_B = \pi/a$ for a chain of particles, the necessary condition to support the waveguide modes is [36,37]

$$a < \lambda/2. \tag{3}$$

Nanoparticles are required to be packed as closely as possible regardless of waveguides made of metallic or dielectric particles [22,29,38]. For atoms, however, the resonance is intrinsic; there is much greater flexibility in the choice of the lattice constant.

The above discussion shows that the one-dimensional lattice spacing cannot be too big. Our numerical result indicates that the lattice spacing cannot be arbitrarily small as well. Physically, as the lattice spacing becomes small, it becomes possible to describe the system with an effective dielectric constant ϵ_{eff} that becomes bigger and bigger as the lattice constant is decreased. Since $k_y^2 = \omega^2\epsilon_{\text{eff}}/c^2 - k_x^2$, it becomes more and more difficult to render k_y^2 negative to localize the electromagnetic wave. Mathematically we find that the imaginary part of the resonance frequency increases when the lattice spacing becomes very small. In this case, it becomes impossible to reduce the radiative loss as described in Appendix C.

Frequency and length dependence. Now we examine the electric field intensity along the chain for different angular frequencies normalized by the resonance angular frequency of the atom as shown in Fig. 2(c). The maximum amplitude occurs around $\omega/\omega_0 = 1.175$. As the frequency moves away, the mode becomes nonpropagating, as is illustrated. The deviation from the single atom resonance comes from the electromagnetic interaction between different atoms constrained by the resonance condition $\mathbf{t}(\mathbf{k})\mathbf{G}(\mathbf{k}) = \mathbf{1}$. We also investigated the transport through atoms for straight lines of two different lengths but the same lattice spacing. The "carrier wave" periodicity remains the same for the different lengths of the chain. Generally, the resonance energy levels form a discrete set for a finite chain of atoms. The spacing between the levels becomes smaller as the length is increased. It is easier to find a resonance energy level closer to the driving frequency.

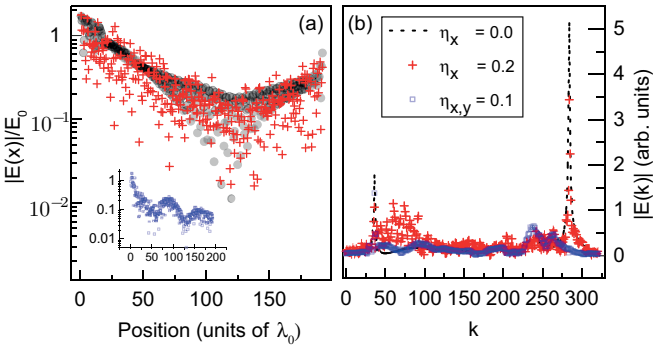

FIG. 3. (Color online) (a) The electric field amplitudes are shown as a function of the position for $N = 320$ atoms of different amounts of positional fluctuations: $\eta_x = 0$ (black solid circle), $\eta_x = 0.2$ (red cross), and $\eta_{x,y} = 0.1$ (blue square in the inset). In (b), the Fourier transform of transverse electric field is shown in units of $2\pi a/N$ for $N = 320$ atoms.

Position fluctuation. We next analyze the possibility of transport through atoms with fluctuations in their positions along the propagating direction (x axis) so that the deviation of the atom from its perfect position is equal to $\eta_x a\xi$. Here ξ is a random number uniformly distributed between -1 and 1 and thus η_x measures the amount of the fluctuation. In addition, we consider the atomic chain with the fluctuation of $\eta_{x,y} = 0.1$ in both the x and y axes independently. The dependence of the electric field E on distance and its Fourier transform is shown in Fig. 3 for different amounts of randomness. The response is quite robust and the waveguide mode persists for all the cases we tested. When the lattice spacing is large, the system does not possess this robustness.

C. Circular chain

Finally we consider "cavities" made from atoms arranged on a circle. For geometric resonances, we have not been able to construct circular cavities with small radiative loss. For intrinsic resonances with smaller lattice spacings, this has now become possible. The distribution of the electric field intensity in real space along the circle is shown in Fig. 4(c) for different frequencies with the external field along different directions. The resonance frequency for propagation is now shifted from that for the straight line; the dependence on the resonance frequency is quite sharp. The mode is excited no matter what direction the external field is.

In Fig. 4(b) we show the Fourier transforms of the electric fields in the radial and the tangential directions for $N = 640$ atoms separated by a lattice spacing $a = 0.6\lambda_0/2\pi$ on the circumferences of a circle after the atom at the top is excited by an external field at an angular frequency $\omega = 1.1$. As can be seen, the field is mainly along the radial direction

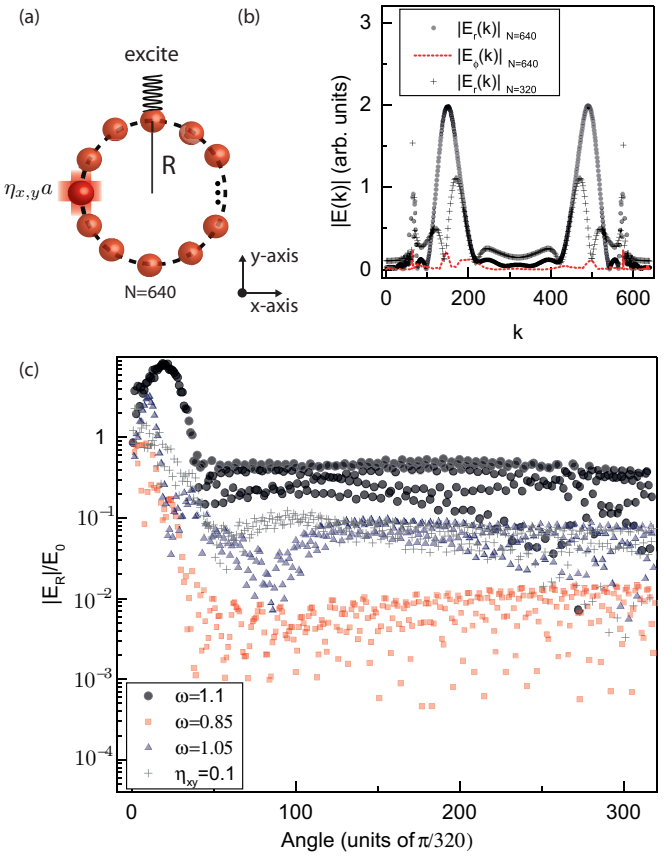

FIG. 4. (Color online) Waveguide mode on the circular atomic chain. (a) The atom at the top is excited by an external electric field resulting in propagating modes in both directions. (b) Fourier transform of radial ($|E_r(k)|$) and tangential ($|E_\phi(k)|$) electric fields as a function of the wave vector $\mathbf{k}$ in units of $2\pi a/N$ for $N = 640$ atoms on the circumferences of a circle at an angular frequency $\omega = 1.1$. (c) Distribution of the radial electric field as a function of the position of the atoms normalized by the lattice constant $a = 0.6\lambda_0/2\pi$ for atoms on the circumferences of a circle with 640 atoms at different frequencies. With the position fluctuation of $\eta_{x,y} = 0.1$ along the x and y direction, respectively, the circular waveguide mode still persists (gray cross).

showing the cavity modes propagating in both directions. We have also studied the system for various numbers of atoms. We show in Fig. 4(b) the Fourier transforms of the electric fields in the radial direction for a smaller number of $N = 320$ atoms separated by the same lattice spacing $a = 0.6$ on the circumferences of a circle after the atom at the top is excited by an external field. The magnitude of the field is now less as is expected. We emphasize that even though this looks similar to the Whispering gallery mode [39], there is no outside wall to confine the wave in the present case. Indeed, there is a high wave-vector "carrier wave" which makes the cavity possible.

D. Discussion

To achieve the waveguide mode along the atomic chain, the controlled patterning of trapped atoms is critical. It can be done either by locating nanoparticles lithographically [40] or through the self-assembly mechanism [41]. In both methods, atoms can be confined within the subwavelength trap associated with the near-field confinement. Another promising way is to confine atoms in a hollow-core fiber [2] or in a two-dimensional photonic crystal [4,32] producing subwavelength lattice potentials.

The present work can be adopted in various systems where the intrinsic atomic resonance plays the role. For cold atoms, alkali-earth-like atoms (e.g., ytterbium or strontium) that have a single principle optical transition due to the total electron spin of zero [42] are suitable. Indeed, our analysis may be extended to the array of atoms with more than one principle resonance. It is also interesting to realize the waveguide mode in the chain of the artificial atoms such as quantum dots [33] or the superconducting building blocks [34] in the microwave domain.

III. CONCLUSION

In conclusion, we demonstrate that the electromagnetic energy can be efficiently transported along a chain of atoms through an atomic resonance with a wavelength of λ_0. We numerically analyze the waveguide mode propagating along a finite chain with appropriate lattice spacing $a \sim 0.6\lambda_0/2\pi$. The efficient subwavelength transportation of electromagnetic energy along the one-dimensional waveguide would provide a main element in integrated nanoscale optical circuits. We believe that ultracold atoms can be localized with subwavelength lattice spacing in the plasmonic nanosphere traps or hollow fibers. Our study of one-dimensional (1D) array structure represents a basic element of complex geometries such as two-dimensional patterning of atoms. For example, it should be interesting to study how the light propagates in the two-dimensional triangular array from one end to the other [43]. Furthermore, a system of two distant atoms connected by a one-dimensional line waveguide [7] or subwavelength-diameter nanofibers [44] reveal interesting transport properties with reduced radiation.

ACKNOWLEDGMENTS

The work was supported by the Hong Kong Research Grants Council (Project No. ECS26300014). S.T.C. acknowledges the hospitality of the Institute for Advanced Studies and the Physics Department of Hong Kong University of Science and Technology where this work was carried out.

APPENDIX A: COUPLING TO ATOMS

We have the usual Hamiltonian $H = -e\mathbf{r}\cdot\mathbf{E}$. The electric field can be expanded in terms of vector spherical harmonics:

$$\mathbf{E}^{\mathbf{J}}(\mathbf{r}) = \sum_{l=0}\sum_{m=-l}^{l} a_{lm}^{JE} N_{lm}^{(J)} + a_{lm}^{JH} M_{lm}^{(J)}. \tag{A1}$$

The vector spherical harmonics are defined as

$$\mathbf{M}_{mn}^{(J)}(x,\theta,\phi) = \frac{\gamma_{mn}}{k}\nabla\times\left[\mathbf{r}\psi_{mn}^{(J)}(x,\theta,\phi)\right], \tag{A2}$$

$$\mathbf{N}_{mn}^{(J)}(x,\theta,\phi) = \frac{\gamma_{mn}}{k}\nabla\times\mathbf{M}_{mn}^{(J)}(x,\theta,\phi). \tag{A3}$$

The scalar spherical functions are given by

$$\psi_{mn}^{(J)}(x,\theta,\phi) = z_n^{(J)}(x) P_n^m(\cos\theta) e^{im\phi}, \tag{A4}$$

where

$$z_n^{(J)}(x) = \begin{cases} j_n(x), & J=1 \\ h_n^{(1)}(x), & J=3 \end{cases} \tag{A5}$$

with $x = kr$ and $n = 0,1,2,\ldots,m = 0,\pm1,...,\pm n$. The superscripts $J = 1$ and $J = 3$ correspond to incoming and outgoing waves. $x_0 = kr_0, \gamma_{mn} = \sqrt{\frac{2n+1}{4\pi n(n+1)}\frac{(n-m)!}{(n+m)!}}$. The electromagnetic field locally is a linear combination of $\mathbf{M} \propto \mathbf{L}Y_{lm}$ and $\mathbf{N}_{lm} \propto \nabla \times \mathbf{M}_{lm}$. These functions all have *total* (orbital plus spin) angular momentum l.

The Hamiltonian is $H = -e\mathbf{r}\cdot\mathbf{E}$. We have $\mathbf{r}\cdot\nabla Y_{lm} = 0, \mathbf{r}\cdot\mathbf{L}Y_{lm} = 0$, $\mathbf{r}\cdot\mathbf{r}Y_{lm} = r^2 Y_{lm}$. Thus, $\mathbf{r}\cdot\mathbf{N}_{1m}$ is the only nonzero term in the dipole approximation. $\mathbf{M} \propto \mathbf{L}Y_{lm}$ contains no radial component, thus this term is not coupled to the atom. To illustrate the physics we consider atoms that exhibit a p-wave resonance so that the atom goes from a state with total angular momentum 0, $|0\rangle$ to a state with angular momentum 1, $|1,m\rangle$ and then reemits a photon. The tangent of the corresponding scattering phase shift exhibits a frequency dependence given by $\tan\delta = 1/(\omega - \omega_0 + i\Gamma)$. The expansion coefficients of the incoming and outgoing fields are related by the $\mathbf{t}$ matrix: $\mathbf{a}^{(3)} = \mathbf{t}\mathbf{a}^{(1)}$. Because the Hamiltonian only involves the electric field and not the magnetic field, there is no coupling involving the coefficients $\mathbf{a}^{(JH)}$. Since we assume a ground state of zero angular momentum and since the Hamiltonian is rotationally invariant, the $\mathbf{t}$ matrix is diagonal in l,m. The $\mathbf{t}$ matrix is related to the tangent of the scattering phase shift δ by $t = \tan\delta/(\tan\delta + i)$. For this resonance the coupling to the electric field is proportional to $\langle 0|\mathbf{E}\cdot\mathbf{r}|1,m\rangle$. Since $\mathbf{N}_{lm}$ is of total angular momentum l, by the Wigner-Eckert theorem, only the terms with $l = 1$ come in.

APPENDIX B: MULTIPLE SCATTERING

The response of the lines of atoms to an external electromagnetic field is treated by multiple scattering theory. The total incoming electric field driving the ith atom $\mathbf{E}_i^{(1)}$ is the sum of the external electric field $\mathbf{E}_i^{\rm ext}$ and the scattered fields from all the other atoms: $\sum_{j\neq i}\mathbf{E}_{ij}^{(\rm sc)}$, i.e., $\mathbf{E}_i^{(1)} = \mathbf{E}_i^{\rm ext} + \sum_{j\neq i}\mathbf{E}_{ij}^{(\rm sc)}$. This incoming field is scattered by the atom and produces a scattered field $\mathbf{E}_i^{(3)}$ that is equal to the $\mathbf{t}$ matrix times the incoming field: $\mathbf{E}_i^{(3)} = \mathbf{t}\mathbf{E}_i^{(1)}$. The field $\mathbf{E}_{ij}^{(\rm sc)}$is equal to the photon propagator $\mathbf{G}_{ij}$ times the scattered field from site j: $\mathbf{E}_{ij}^{(\rm sc)} = \mathbf{G}_{ij}\mathbf{E}_j^{(3)}$. To summarize, we get the set of linear equations

$$\mathbf{E}_i^{(3)} - \sum_{j\neq i}\mathbf{G}_{ij}\mathbf{t}\mathbf{E}_j^{(3)} = \mathbf{t}\mathbf{E}_i^{\rm ext}. \tag{B1}$$

The photon propagator [45] in terms of the vector potential A_μ is $D_{\mu\nu} = -g_{\mu\nu}/(k^2 + i\epsilon)$. Because $\phi = 0$, we need not worry about $\mu = \nu = 0$. In classical E&M, we worry about the Green's function $G(r) = \int d^3r/(k^2 - \omega^2)$. This is identical to the Fourier transform of the photon propagator.

APPENDIX C: SMALL LATTICE SPACING

In this appendix, we describe the physics when the lattice spacing is small. The multiple scattering equation is

$$\mathbf{E}_i^{(3)} = \mathbf{t}_i\left[\sum_{j\neq i}\mathbf{G}_{ij}\mathbf{E}_j^{(3)} + \mathbf{E}_i^{\rm ext}\right]. \tag{C1}$$

We consider a line of atoms line up along the z axis. Then the Green's function is particularly simple [46]. G is diagonal in m and is given by

$$G_{ij}^{n,\nu} = C_0 \sum_{q=0}^{\min(n,\nu)} i^p C'_p a_q h_p(k_0|R_{ij}|)$$

for R on both the left and the right, where $p = n + \nu - 2q$, $C'_p = n(n+1) + \nu(\nu+1) - p(p+1)$, and a is the Wigner $3j$ symbol. For the present approximation, $n = \nu = 1$. We thus get ($C'_2 = 4 - 6 = -2$, $C'_0 = 4$)

$$G_{ij}^{1,1} = C_0[2a_0 h_2(k_0 R_{ij}) + 4a_1 h_0(k_0 R_{ij})].$$

For an infinite chain, $E_l \propto \exp(ikla)$. We need

$$G(k) = \sum_{R\neq 0} G(R) = C_0[2a_0 g_2(k) + 4a_1 g_0(k)],$$

where $g_n(k) = \sum_{R\neq 0}\exp(ikR)h_n(k_0 R)$. The above equation becomes

$$\mathbf{E}(k) = \mathbf{t}[\mathbf{G}(k)\mathbf{E}(k) + \mathbf{E}^{\rm ext}(k)]. \tag{C2}$$

The resonance condition is

$$\mathbf{1} = \mathbf{t}\mathbf{G}.$$

We look at the small a limit. Take $h = j + iy$, $h_0(x) = [\sin(x) - i\cos(x)]/x = -i[i\sin(x) + \cos(x)]/x = -i\exp(ix)/x$. Define $x_j = ja$. For example, for $n = 0$, $h_0(x) = -i\exp(ix)/x$,

$$\begin{aligned} g_0(k) =& 2\sum_{j\neq 0}(\Delta x_j)\exp(ikx_j)h_0(k_0|x_j|)/a \\ =& \sum_{j>0}(\Delta x_j)\{\exp[i(k+k_0)x_j] \\ &+ \exp[i(-k+k_0)x_j]\}/(k_0 x_j a) \\ \approx& \int_a^\infty dx\{\exp[i(k+k_0)x] \\ &+ \exp[i(-k+k_0)x]\}/(k_0 x a). \end{aligned}$$

Both the real and the imaginary parts of g scales as $\ln(a)/a$. This dependence will also dominate $1 - tG$. Thus the imaginary part of $E_s = tE_i/(1 - tG)$ will not be small in the small a limit.

APPENDIX D: POYNTING VECTOR

The total field is a sum of the scattered field from each of the atoms at position r_i: $\mathbf{E}(r) = \sum_i E_m^{\rm sc}(i)\mathbf{X}_m(r - r_i)$ where $\mathbf{X}$ is the vector spherical harmonics $\mathbf{N},\mathbf{M}$. We express our results in terms of the Fourier coefficients of the scattered field: $E_m^{\rm sc}(i) = \sum_k E_m^{\rm sc}(k)e^{-ikz_i}/\sqrt{N}$, where $\mathbf{k}$ is the reciprocal

lattice vector of the 1D lattice. We get, using the Poisson summation formula (to simplify the notation, we pick the z axis to be along the chain here),

$$\mathbf{E} = \sum_{\mathbf{K},\mathbf{k}} E_m^{\mathrm{sc}}(\mathbf{k}) e^{i(K-k)z-\kappa_\perp r_\perp} \mathbf{X}_m(\mathbf{K}-\mathbf{k})/\sqrt{N},$$

where $\mathbf{K}$ and $\mathbf{k}$ are along the chain. Here $\kappa_\perp = [-\omega^2/c^2 + (\mathbf{K}-\mathbf{k})^2]^{1/2}$ is the imaginary transverse wave vector and $\mathbf{K}$ is a reciprocal lattice vector of the lattice. $\mathbf{X}_m(p) = \int d^3r' e^{-ipr'} \mathbf{X}_m(r')(2\pi)^3/V$. The magnetic field is given by $\mathbf{B} = \mathbf{H}\mu_0 = \nabla \times \mathbf{E}/i\omega = (\mathbf{K}-\mathbf{k}) \times \mathbf{E}/\omega$. The Poynting vector is given as

$$\begin{aligned}\mathbf{P} &= \mathbf{E} \times \mathbf{H}^* \\ &= (\omega\mu_0)^{-1} \sum_{K,k} e^{-2\kappa_\perp r_\perp} (\mathbf{K}-\mathbf{k}) |E_m^{\mathrm{sc}}(k) X_m(K-k)|^2/N.\end{aligned}$$

[1] C. A. Christensen, S. Will, M. Saba, G.-B. Jo, Y.-i. Shin, W. Ketterle, and D. Pritchard, Phys. Rev. A **78**, 033429 (2008).

[2] M. Bajcsy, S. Hofferberth, T. Peyronel, V. Balic, Q. Liang, A. S. Zibrov, V. Vuletic, and M. D. Lukin, Phys. Rev. A **83**, 063830 (2011).

[3] M. Bajcsy, S. Hofferberth, V. Balic, T. Peyronel, M. Hafezi, A. S. Zibrov, V. Vuletic, and M. D. Lukin, Phys. Rev. Lett. **102**, 203902 (2009).

[4] C. L. Hung, S. M. Meenehan, D. E. Chang, O. Painter, and H. J. Kimble, New J. Phys. **15**, 083026 (2013).

[5] A. Goban, C. L. Hung, S. P. Yu, J. D. Hood, J. A. Muniz, J. H. Lee, M. J. Martin, A. C. McClung, K. S. Choi, D. E. Chang, O. Painter, and H. J. Kimble, Nat. Commun. **5**, 3808 (2014).

[6] D. Dzsotjan, A. S. Sørensen, and M. Fleischhauer, Phys. Rev. B **82**, 075427 (2010).

[7] J. T. S. S. Fan, Opt. Lett. **30**, 2001 (2005).

[8] D. E. Chang, L. Jiang, A. V. Gorshkov, and H. J. Kimble, New J. Phys. **14**, 063003 (2012).

[9] R. Halir, P. J. Bock, P. Cheben, A. Ortega-Monux, C. Alonso-Ramos, J. H. Schmid, J. Lapointe, D.-X. Xu, J. G. Wangueemert-Perez, I. Molina-Fernandez, and S. Janz, Laser Photonics Rev. **9**, 25 (2015).

[10] *Selected Papers on Subwavelength Diffractive Optics*, edited by J. N. Mait and D. W. Prather (Society of Photo-Optical Instrumentation Engineers, Bellingham, WA, 2001).

[11] P. Yeh, Opt. Commun. **26**, 289 (1978).

[12] E. B. Grann, M. G. Moharam, and D. A. Pommet, J. Opt. Soc. Am. A **11**, 2695 (1994).

[13] S. J. Wilson and M. C. Hutley, Opt. Acta **29**, 993 (1982).

[14] M. E. Motamedi, W. H. Southwell, and W. J. Gunning, Appl. Opt. **31**, 4371 (1992).

[15] R. Halir, P. Cheben, S. Janz, D.-X. Xu, I. Molina-Fernandez, and J. G. Wangüemert-Pérez, Opt. Lett. **34**, 1408 (2009).

[16] M. C. Y. Huang, Y. Zhou, and C. J. Chang-Hasnain, Nat. Photonics **1**, 119 (2007).

[17] P. Cheben, P. J. Bock, J. H. Schmid, J. Lapointe, S. Janz, D.-X. Xu, A. Densmore, A. Delâge, B. Lamontagne, and T. J. Hall, Opt. Lett. **35**, 2526 (2010).

[18] P. J. Bock, P. Cheben, J. H. Schmid, J. Lapointe, A. Delâge, D.-X. Xu, S. Janz, A. Densmore, and T. J. Hall, Opt. Express **18**, 16146 (2010).

[19] J. Wang, I. Glesk, and L. R. Chen, Opt. Express **22**, 15335 (2014).

[20] A. Maese-Novo, R. Halir, S. Romero-García, D. Pérez-Galacho, L. Zavargo-Peche, A. Ortega-Moñux, I. Molina-Fernández, J. G. Wangüemert-Pérez, and P. Cheben, Opt. Express **21**, 7033 (2013).

[21] E. Ozbay, Science **311**, 189 (2006).

[22] W. L. Barnes, A. Dereux, and T. W. Ebbesen, Nature (London) **424**, 824 (2003).

[23] R. Zia, J. A. Schuller, A. Chandran, and M. L. Brongersma, Mater. Today **9**, 20 (2006).

[24] S. A. Maier, P. G. Kik, H. A. Atwater, S. Meltzer, E. Harel, B. E. Koel, and A. A. G. Requicha, Nat. Mater. **2**, 229 (2003).

[25] S. I. Bozhevolnyi, J. Erland, K. Leosson, P. M. W. Skovgaard, and J. M. Hvam, Phys. Rev. Lett. **86**, 3008 (2001).

[26] P. Berini, Phys. Rev. B **61**, 10484 (2000).

[27] J. R. Krenn and J. C. Weeber, Philos. Trans. R. Soc. London, Ser. A **362**, 739 (2004).

[28] K. Tanaka and M. Tanaka, Appl. Phys. Lett. **82**, 1158 (2003).

[29] S. A. Maier, *Plasmonics: Fundamentals and Applications* (Springer, New York, 2007).

[30] J. Du, S. Liu, Z. Lin, J. Zi, and S. T. Chui, Phys. Rev. A **79**, 051801 (2009).

[31] M. Gullans, T. G. Tiecke, D. E. Chang, and J. Feist, Phys. Rev. Lett. **109**, 235309 (2012).

[32] A. González-Tudela, C. L. Hung, D. E. Chang, J. Cirac, and H. J. Kimble, Nat. Photonics **9**, 320 (2015).

[33] R. C. Ashoori, Nature (London) **379**, 413 (1996).

[34] A. Wallraff, D. I. Schuster, A. Blais, L. Frunzio, R. S. Huang, J. Majer, S. Kumar, S. M. Girvin, and R. J. Schoelkopf, Nature (London) **431**, 162 (2004).

[35] P. C. Waterman, Proc. IEEE **53**, 805 (1965).

[36] A. L. Burin, H. Cao, G. C. Schatz, and M. A. Ratner, J. Opt. Soc. Am. B **21**, 121 (2004).

[37] G. S. Blaustein, M. I. Gozman, O. Samoylova, I. Y. Polishchuk, and A. L. Burin, Opt. Express **15**, 17380 (2007).

[38] M. Quinten, A. Leitner, J. R. Krenn, and F. R. Aussenegg, Opt. Lett. **23**, 1331 (1998).

[39] L. Rayleigh, *Rayleigh: The Theory of Sound, 1894—Google Scholar* (republished by Dover, New York, 1945).

[40] P. Nagpal, N. C. Lindquist, S.-H. Oh, and D. J. Norris, Science **325**, 594 (2009).

[41] J. A. Fan, C. Wu, K. Bao, J. Bao, R. Bardhan, N. J. Halas, V. N. Manoharan, P. Nordlander, G. Shvets, and F. Capasso, Science **328**, 1135 (2010).

[42] J. E. Sansonetti and W. C. Martin, J. Phys. Chem. Ref. Data **34**, 1559 (2005).

[43] C. Becker, P. Soltan-Panahi, J. Kronjager, S. Dörscher, K. Bongs, and K. Sengstock, New J. Phys. **12**, 065025 (2010).

[44] L. Tong, R. R. Gattass, J. B. Ashcom, S. He, J. Lou, M. Shen, I. Maxwell, and E. Mazur, Nature (London) **426**, 816 (2003).

[45] F. Mandl and G. P. Shaw, *Quantum Field Theory* (Wiley, New York, 2013).

[46] Y.-l. Xu, Appl. Opt. **34**, 4573 (1995).